COMITATO NAZIONALE PER L'ENERGIA NUCLEARE
Laboratori Nazionali di Frascati

LNF-73/59
8 Ottobre 1973

H. Ogren, A. Mariani and D. Bisello: MEA-MAGNETIC FIELD MEASUREMENTS.

Servizio Documentazione
dei Laboratori Nazionali di Frascati del CNEN
Casella Postale 70 - Frascati (Roma)

Laboratori Nazionali di Frascati del CNEN
Servizio Documentazione

LNF-73/59
8 Ottobre 1973

H. Ogren, A. Marini and D. Bisello: MEA-MAGNETIC FIELD MEASUREMENTS. -

1. - INTRODUCTION. -

The magnet experiment at Adone (MEA)[1] will provide a comprehensive study of e^+e^- interactions, including pion and kaon form factors, e^+e^- and $\mu^+\mu^-$ final state cross sections with charge recognition, and the cross sections for all hadron final states with charged multiplicity greater than or equal to two.

The experimental apparatus as shown in Fig. 1 consists of a mixture of counters, narrow gap and wide gap chambers, and proportional chambers. The prominent feature, of course, is a large solenoid magnet with a radius of one meter and a length of two meters. This solenoid is mounted transversly to the e^+e^- beams and has a maximum central field value of $\sim$ 5000 gauss. Without a compensation system, therefore, each of the beams would see $\sim$10,000 gauss-meters of field integral. A pair of compensator magnets (Fig. 2) attached in series electrically with the main bobbin surround about 50% of the beam path inside the solenoid and must reduce the net field integral to zero.

This paper reports on the measurement of the above mentioned field integral and, in addition, on a separate, but equally important measurement, that of the field throughout the entire solenoid volume. This later field map will be needed for an accurate momentum determination of the final state particles.

2. - INTEGRAL MEASUREMENT. -

In order for the magnet-compensator system to have a negligible effect on the stability of the stored beams two basic conditions on the magnetic fields must be satisfied by the system:

(1) $$B(s) = B(-s)$$

(2) $$\int B(s)\,ds = 0$$

where s is a coordinate measured from the center of the magnet along the ideal beam orbit.

Condition (1) can be established with careful construction techniques and has been verified by direct measurements (see section 4). This condition is required to insure that there will be no net beam displacement even when (2) is satisfied.

Condition (2), which implies no net change in angle of the beams passing through the system, must be satisfied not only along the beam axis, but also for vertical and horizontal displacements from this axis by $\pm$ 2 cm. Acceptable deviations from this condition, $\int B(s)ds = 0$, can be expressed as maximum gradients of the integral for displacements parallel to the axis in x or y directions (generalized coordinate ξ) and written

$$\int B ds = C + G\,\xi + H\,\xi^2 + M\,\xi^3$$

These maximum acceptable values have been determined by Amman(2).

Very roughly, we can describe the limitations on the gradients as follows: a non-zero integral C results in a displacement of the equilibrium orbit vertically or horizontally. Restricting the maximum displacement anywhere in the machine to be 2 mm, one can calculate $C \leq 2.5$ Gs. m.

The gradient G is directly related to the focusing in either plane and is restricted by demanding that $d\nu / \nu_0$ be less than 10^{-3}; this gives $G < 0.7$ Gs. m/cm.

The constant H determines the amount of sextupole term introduced by the MEA system. By specifying that this be less than 20% of the integrated sextupole term of Adone, one obtains the limit, $H \leq \leq 0.7$ Gs. m/cm^2.

Similarly terms M and higher order can be restricted by specifying that they do not exceed the octupole or higher multipole terms already present in Adone. In the case of M this gives $M \leq 0.4$ Gs. m/cm^4.

Summarizing these restrictions:

$$\int Bds(\text{error}) \leq 2.5 \text{ Gs.m}$$

$$G \text{ (quadrupole)} \leq 0.7 \text{ Gs.m/cm}$$

$$H \text{ (sextupole)} \leq 0.7 \text{ Gs.m/cm}^2$$

$$M \text{ (octupole)} \leq 0.4 \text{ Gs.m/cm}^4 .$$

Since the active length of the beam-magnet interaction is about 3 meters, the above stated conditions on the integral error imply an absolute measure of B better than 0.8 gauss over the entire range -5000 gauss to +5000 gauss and a relative precision of ~ 0.2 gauss for displacement off-axis. The difficulties implied by these numbers led us to develope an instrument that could measure accurately and directly the integral itself instead of the field components. This field integrator has been described in a previous letter[3].

The field integral along a length of 3 meters is determined by measuring the force on a current carrying rod (positioned along the beam) and gives an absolute precision better than $\pm$ 0.5 gauss-meters. Noise reduction is accomplished by extraction of the modulated current signal with a lock-in amplifier. Absolute calibration of the instrument was provided by a known field produced by a coil attached to the integrator support, giving a test point at 20 gauss-meters.

Positioning of the integrator was accomplished with a hydraulic system for vertical, horizontal and rotational movements. Positions were determined by optical surveying to ~ 1 mm.

The main magnet bobbin and the compensator magnets (see Figs. 1,2) were connected in series electrically, so that, apart from small design errors and effects of saturation, the field integral was expected to be near zero for all values of the main current. Small corrections to this integral (about 10% of the compensator field) could be made with an additional power supply attached to a correction coil built into the compensator magnets.

A series of preliminary measurements resulted in some basic restructuring of the compensator magnet design. The compensator field was lowered by $\sim 30\%$ by replacing 15 mm of iron in the magnetic circuit with aluminum (see Fig. 2)[4]. Further, gradients present in the central field were reduced by strategically placed soft iron bars. (see section 3),.

When these changes were made, and in addition two soft iron

plates were positioned near the main bobbin to simulate the effects of the two quadrupoles in the storage rings, the integral could be nulled using the correction coils over the entire range 0-4500 amp. Fig. 3 showes the voltage reference values for the correction coil power supply (10 V_{ref}= 500 amp.) as a function of the main coil current. The reproducibility of all points was $< 0.5\%$ and the sensitivity was the following:

0.3 gauss-meters/amp. (main bobbin)

0.08 gauss-meters/mV (correction coil)

These points are listed in Table I.

At the same time, in order to more clearly understand the internal fields, a series of measurements along the beam axis were made using a Hall probe (see section 4). This field profile along the beam axis is shown at 4500 amps in Fig. 4. The field integrals due to the bobbin and the compensators could then be calculated separately (but not very precisely) and studied as a function of the main power supply current. These separate field integrals are shown in Fig. 5. Notice that for these curves the correction coil system was not used in order to show the effects of saturation in the compensators. Of course, with the correction coil current turned on, the compensator integral curve is linear, matching that of the bobbin, and these two components sum to zero.

3. - GRADIENT MEASUREMENTS. -

As was stated previously, the presence of field gradients introduced by the compensator-magnet system poses a potentially serious problem for Adone. Unfortunately these gradients, mostly due to geometrical and saturation effects, can be much more difficult to correct than the field integral deviations, which simply required the addition of a separate correction coil system. Furthermore, the limits on the gradient terms were very stringent, making their measurement difficult. Again, the field integrator described previously was used for these measurements. Displacements of the integrator parallel to the beam axis, both horizontally and vertically, were accomplished by an hydraulic system and measured by optical surveying.

The first gradient measurements were made after the compensators had been modified (shorter magnetic circuit) and indicated the presence of large gradients. Fig. 6a, b, shows the results of two measurements at currents of 2000 amp and 4300 amp with the condition $\int B_y dz =$

$= 0$ at $x = 0$, $y = 0$. We have also indicated in the figure the multipole expansion fitted to these points. The values of the various multipole terms are given in Table IIa. In both cases the terms were an order of magnitude higher than acceptable. From the table one can see that the main effect was a large sextupole term. By direct measurement it was confirmed that the central field of the compensator itself was responsible for this large sextupole term and not, for example, the fringe fields of the bobbin or compensators.

The most obvious way to attempt to correct these gradients was by reshaping the pole faces. However, we found that due to the long gap length and small pole height it was impossible to produce significant effects with simple changes in the pole shape. Fortunately another simple solution was found when it was discovered that four soft iron bars arranged as in Fig. 7 produce an almost pure sextupole field of the opposite sign of that introduced by the compensators. The magnitude of the sextupole field, which depends on the external field and the radii and relative position of the cylinders, was adjusted experimentally to cancel the existing sextupole term. Since the applied sextupole field is expected to scale as the field of the compensator it could also be expected to follow effects of compensator saturation.

How well this cancellation worked (as a function of magnet current) is shown in Fig. 8a-c. The smooth lines are the multipole fits. Table II b gives the values of these multipole terms for each current value and, in addition, Fig. 9 showes the largest of these terms plotted for each current value. As can be seen from the figure, within the fitting errors, the terms satisfy the limits stated previously and it was felt that Adone could tolerate the largest excursions indicated. Moreover, the simplicity of the correction system had many advantages for the ease of operation of Adone.

4. - BEAM AXIS PROFILE AND BEAM TRAJECTORIES. -

As was stated previously, a measurement of the magnetic field at points along the beam axis was also performed under the null field integral condition for seven different values of the magnet current. These measurements allowed us to verify the symmetry of the magnet system, understand the fringe fields of the main bobbin, calculate the relative contributions of the various points of the system to the total field integral, plot the electron-positron trajectories, and finally (as will be mentioned in the following section) map a region of interest for momentum reconstruction that was not covered by the field mapping device.

Measurements were recorded automatically on-line to a PDP8 computer and written on magnetic tape for later analysis, using hardware, techniques, and software that will be described later.

The measurement of the principal field values along the beam axis at ~1 cm intervals required about 5 minutes for each current value. A profile at 4500 amp is shown in Fig. 4. From this measurement the electron trajectory in Fig. 10 was calculated. In addition Table III indicates the central displacements of the e^+e^- beams for three values of momentum calculated from similar magnetic profiles and trajectories for each of the seven currents measured. Since the vertical height of the vacuum chamber is ~4 cm these beam displacements are quite acceptable. Notice also that in Fig. 10 the final displacement of the beam is zero (within the field measurement errors) indicating that the symmetry conditions have been fulfilled. This is found to be true, of course, at all current values measured.

5. - INTERNAL FIELD MAP. -

5.1. - Field measurements. -

Accurate momentum analysis of events photographed in the magnetic volume of MEA requires a precise determination of the field components at all points inside the solenoid. In order that the field measurements be compatible with the required momentum precision of MEA, $\Delta p/p \sim 0.5\%$, the value of the principal component of the magnetic field must also be measured with this precision.

The field was mapped using a self-propelled Hall probe measuring head whose coordinates and associated field component values were simultaneously read out by a PDP8 computer and written on magnetic tape. The mapper head, shown in Fig. 11 carried 3 orthogonal Hall probes. The displacement mechanisms for movements along the solenoid axis (z) and azimuthal angle (φ) were driven by electric motors with automatic reversals at adjustable end points. The r position on the other hand was controlled by a hydraulic system. The measurement intervals were the following:

z (-1.90 to +1.90 meters)

r (0.10 to 0.95 meters)

ϕ (0.53 to 2.3 rad, 3.7 to 5.4 rad)

Positions of all three coordinates were measured with three scanning table string digitizers to a precision of better than 1 mm for all volume points.

The Hall probes and associated electronics have been described previously[5]. All three probes, having thermostatically controlled heaters, were calibrated by us against a Varian Hall probe. The calibration curves of the low field probes (B_r and B_ϕ) in the range 0-2000 gauss were fit with a linear function resulting in maximum deviations from the fit of 0.5 gauss and a standard deviation of 0.2 gauss. The calibration curve of the high field probe (B_z) yielded a linear fit in the range 2000-5000 gauss, with a maximum deviation of 1.5 gauss and a standard deviation of 0.7 gauss. The long term stability of the probes and associated electronics was better than $\pm$ 2 gauss and the absolute calibration was determined to be better than 0.1% at all high field values.

The measuring head velocity was typically $V_z = 1$ cm/sec, $V_r = 0.05$ cm/sec, $V\varphi = 50$ mrad/sec and the sampling rate was about 1 Hz. Thus a complete measurement of one half the volume (upper $\varphi = 0.53$ to 2.3 rad or lower $\varphi = 3.7$ to 5.4 rad) consisting of 2000 measurements could be completed in about one half hour.

Maps of both upper and lower sections were completed for the following currents: 2000, 3000, 3500, 3700, 4000, 4300, and 4500 Amps. All of these measurements were made with the compensators giving a zero field integral and, in addition at 4000 Amp a displaced value of the correction current was used to measure our sensitivity to this parameter.

Figs. 12a-f show the principal projections of the field map at 4500 Amp. Notice that the field component B_z is uniform to within 15% for r = 0.5 - 1.0 meters, while for small z and small r where the influence of the compensators is strong, there is a reduction of up to 30%. Uniformity in φ is very good, better than 2% except for points very near the compensators.

5.2.- Field analysis and fitting procedures.-

Several fitting routines were used to try to find an analytic fit to the measured fields. A multipole expansion in cartesian coordinates, involving terms up to 8^{th} order and simultaneously fitting all three components failed to give (even at 8^{th} order) a ΔB (average field deviation from fit) better than 80 gauss for a central field of 3000 gauss. Similarly a cylindrical geometry multipole expansion involving only terms to the second order, (of the form $(1+z+z^2)(1+r^2)(1+\cos^2\varphi)$) failed to fit the B_z component alone, again with a $\Delta B \sim 80$ gauss.

Rather than expanding the number of term and fitting parameters for the cylindrical multipole fit, it was then decided to tailor the fitting functions to the existing geometry, i.e., take into account expli-

citly the compensator fringe fields, a small gap in the main field windings where the two halves of the bobbin join, and the two large holes in the iron end caps. This was accomplished by adding to the cylindrical multipole fit an expression for the field due to two magnetic dipoles fixed along the beam axis with adjustable symmetric displacements along the beam axis and adjustable symmetric dipole constants. The result of this addition was a much better fit to the field near the compensators and $\Delta B \sim 35$ gauss.

In addition three current loops were added; one at the central plane with a fixed radius of 1.06 meters to simulate the missing winding, and one at either end of the solenoid with a radius of 0.45 meters to simulate the effect of the holes in the end caps. In both cases the currents (symmetric in the case of the end caps) were adjustable. The result of these additional two parameters was to lower $\Delta B \sim 20$ gauss. Finally, by studying the fitting deviations near the compensators, two additional functional forms with adjustable scaling coefficients were added, bringing the total number of fitting parameters to 20 and reducing ΔB to ~ 10 gauss for a central field 3000 gauss, i.e., 0.3% average deviation. The explicit functions are shown in Table IV.

Two other details were necessary to complete the fitting procedure. There is a region of space described by two cones extending in $\pm$ z directions with apexes at z = 0 and bases occupying essentially the entire opening in the end caps that does not contain chambers for momentum analysis and therefore was not included in the fit. In addition the mapping device used had a minimum r displacement of ~ 10 cm, while for the momentum reconstruction we need to know the field along beam axis ($\varphi = 0, \pi$; r = 0-0.2 m) due to the extended source distribution. For this reason we included in the fit. 10 field measurements taken during the beam profile measurements (with the same Hall probe that measured the B_z component) extending $\pm$ 0.18 meters in either direction along the beam axis and we gave them a weight of 10 with respect to the other field values.

The complete fitting program contained 20 parameters (listed in Table IV), occupied 300 K for each half of the magnet being fit, and required typically 1.6 minutes on a IBM 360/75 computer to fit each component independently for 2000 field points[6]. Table IV contains the fitting parameter results for the 3 components and seven current values. Notice that the upper and lower halves were fit independently, and that also each of the three components was fit independently. For each fit $\Delta B = \sqrt{\Sigma (B_{meas} - B_{cal})^2}$/number of points, is indicated. For the principle component this average fitting error is typically 0.3%. This figure represents a maximum for the momentum reconstruction error due to magnetic field uncertainty and is well below estimated uncertainties due to scanning errors, fiducial measurements, etc.

ACKNOWLEDGEMENTS. -

As is the case with most reports of this type, the results are due to the combined efforts of many individuals. In the case of MEA and these magnetic field measurements this is especially true, considering the history of development beginning in 1967 and the large number of people directly involved with the initial design, the mechanical and electrical aspects, the storage ring interactions, and finally the measurements themselves.

There has been a continual and fruitful interaction between the MEA group and the Adone group headed by Prof. Amman and the magnet group headed by Prof. Sacerdoti. In particular we have benefited from the continual support of the engineering section of Adone lead by Eng. Cattoni the long hours of work by A. Bernardi of the magnet group, and the assistence of our experimental technician G. Schina.

Within the MEA group particular mention should be made of the contributions of Dr. Carlo Costa during the initial calibrations of our measurement apparata, Francesco Ronga and Marcello Piccolo for the design and testing of the prototype field integrator, and Franco Felicetti and Vittorio Silvestrini for helpful advice on both technical and administrative details.

REFERENCES. -

(1) - W. Ash, D. Grossman, G. Matthiae, G. P. Murtas, M. Nigro, G. K. O'Neill, G. Sacerdoti, R. Santangelo, D. Scannicchio and E. Schiavuta, A Magnetic Analyzer to be used for Adone Colliding Beam Experiments, Frascati Internal Report LNF-69/2 (Int.) (1969).

(2) - F. Amman, Campo Magnetico MEA - Tolleranze Ammesse, Memorandum Interno Adone, ME-27 (1969).

(3) - A. Cattoni, M. Piccolo and F. Ronga, A High Sensitivity Method for Measuring Magnetic field Integrals, Nuclear Instr. and Meth. 96, 573 (1971).

(4) - We would like to thank Prof. Sacerdoti for suggesting and carrying out this modification and for continual help and advice on all the compensator problems.

(5) - M. Placidi, F. Soso e M. Vescovi, Un misuratore di Campo Magnetico a sonde di Hall, Frascati Report LNF-68/30 (1968).

(6) - For additional details refer to Tesi di Laurea in Fisica, A. Marini, Roma (1973) (unpublished).

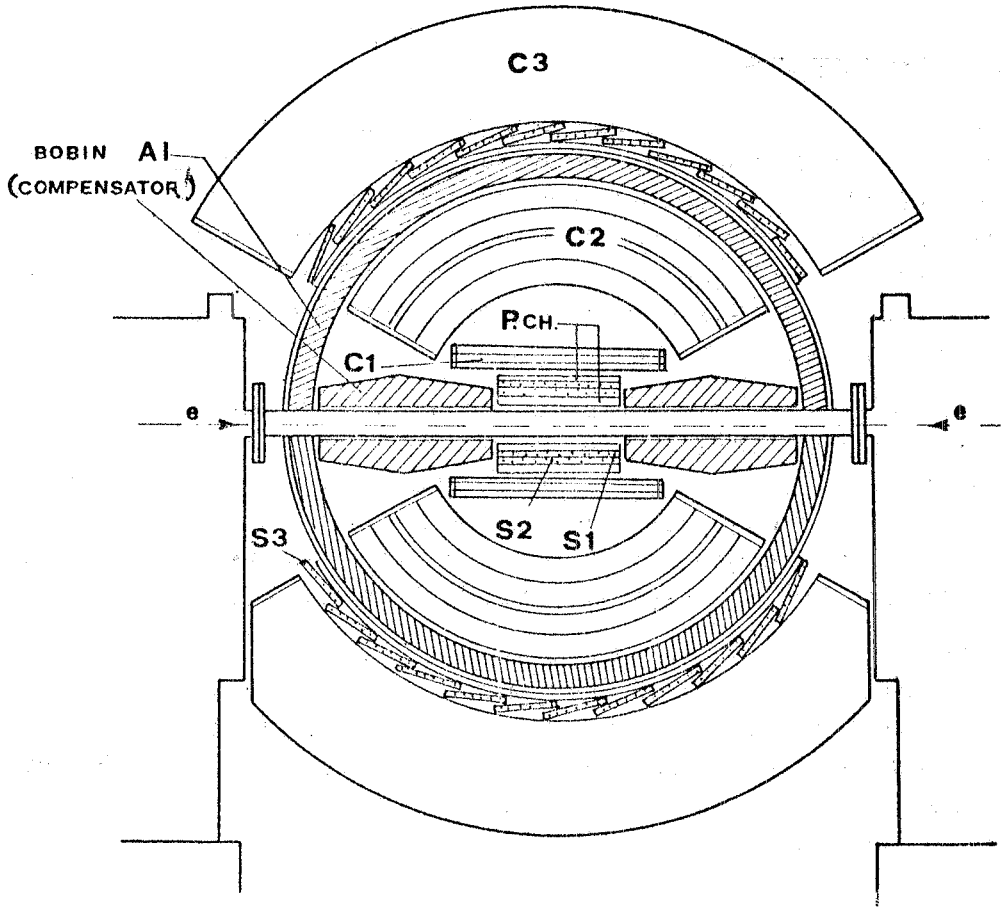

FIG. 1 - MEA Experimental Apparatus - C3: Cylindrical iron-lead shower chambers; S3, S2, S1: scintillator counters; C2: wide gap spark chamber, P.CH: Multiwire proportional chambers.

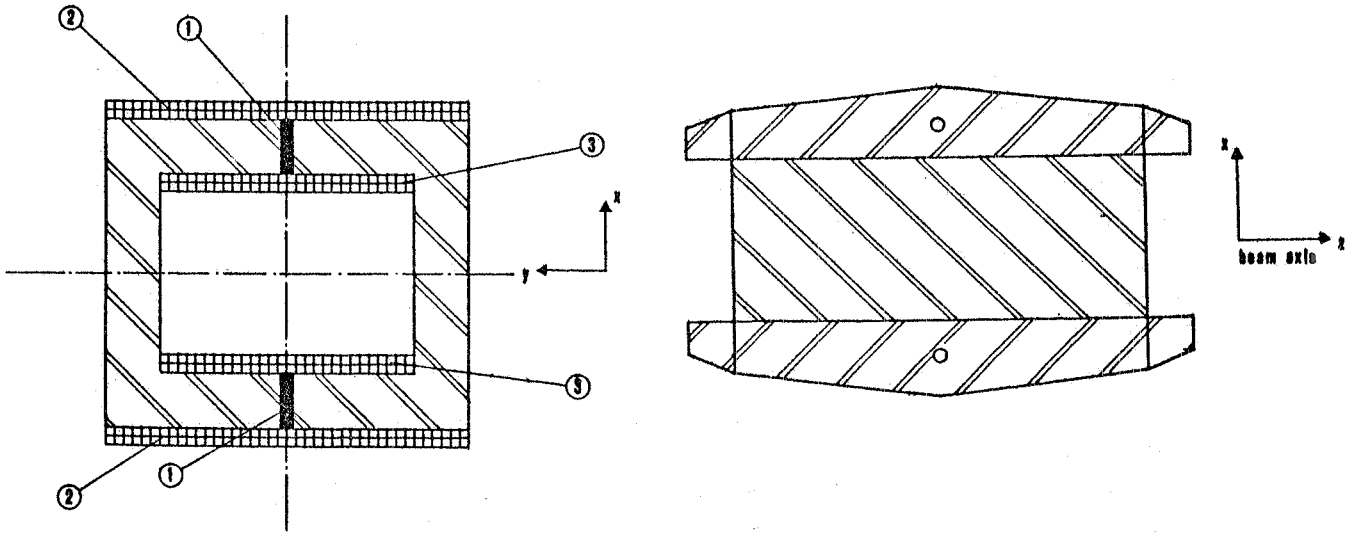

FIG. 2 - Compensator construction details. (1) Aluminum magnetic circuit gap (2) external coils (3) internal and correction coils.

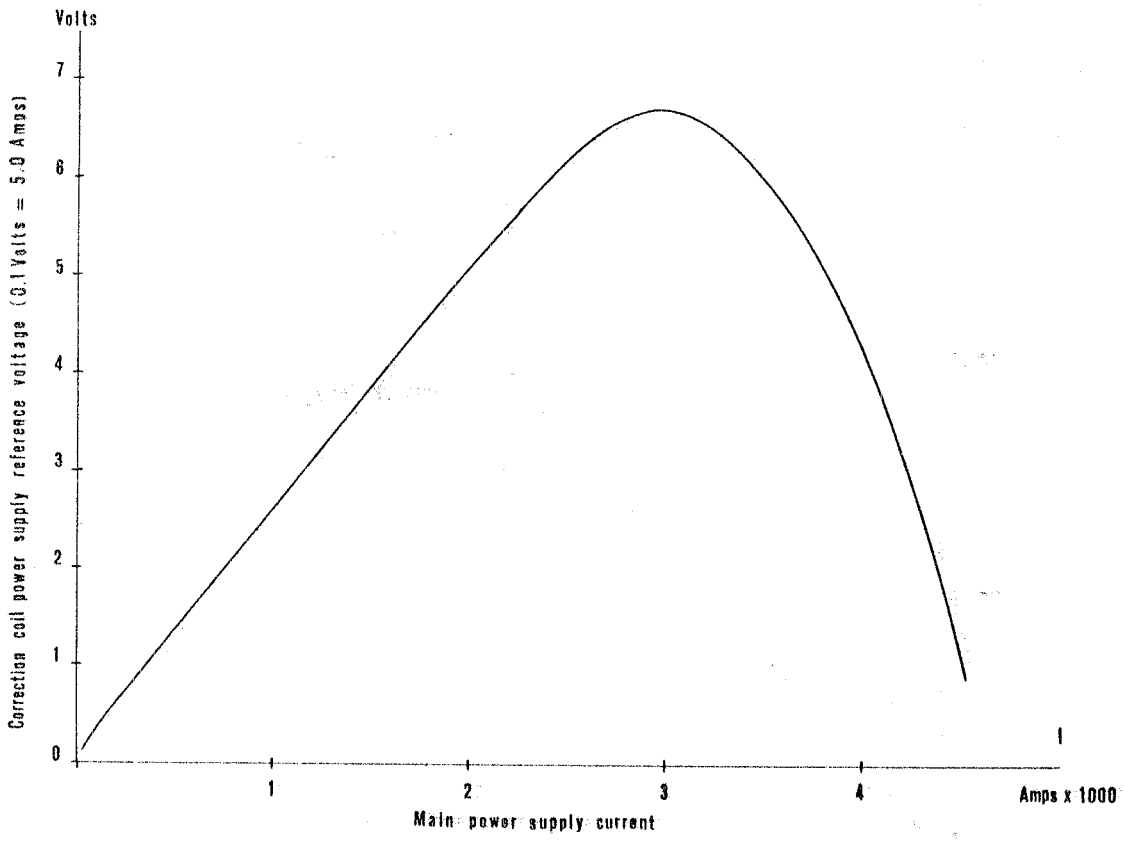

FIG. 3 - Compensator correction coil power supply reference voltage vs. main power supply current for zero field integral.

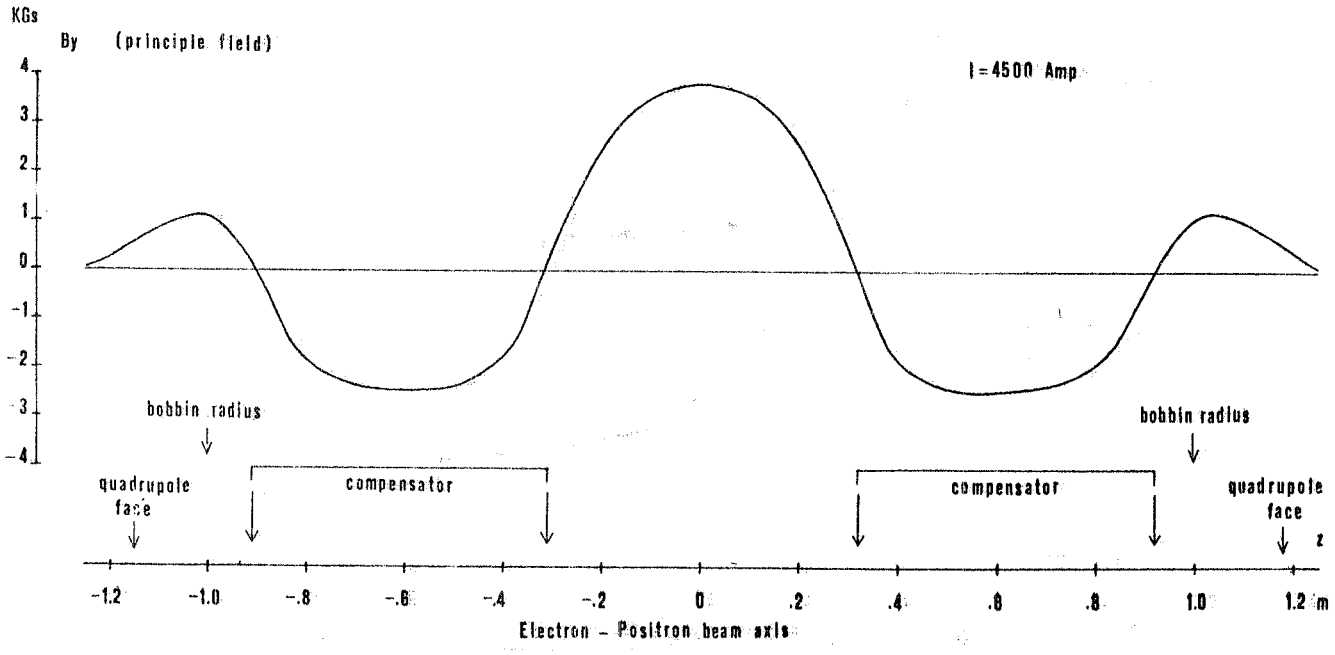

FIG. 4 - Transverse field profile along beam axis for a main power supply current of 4500 amp.

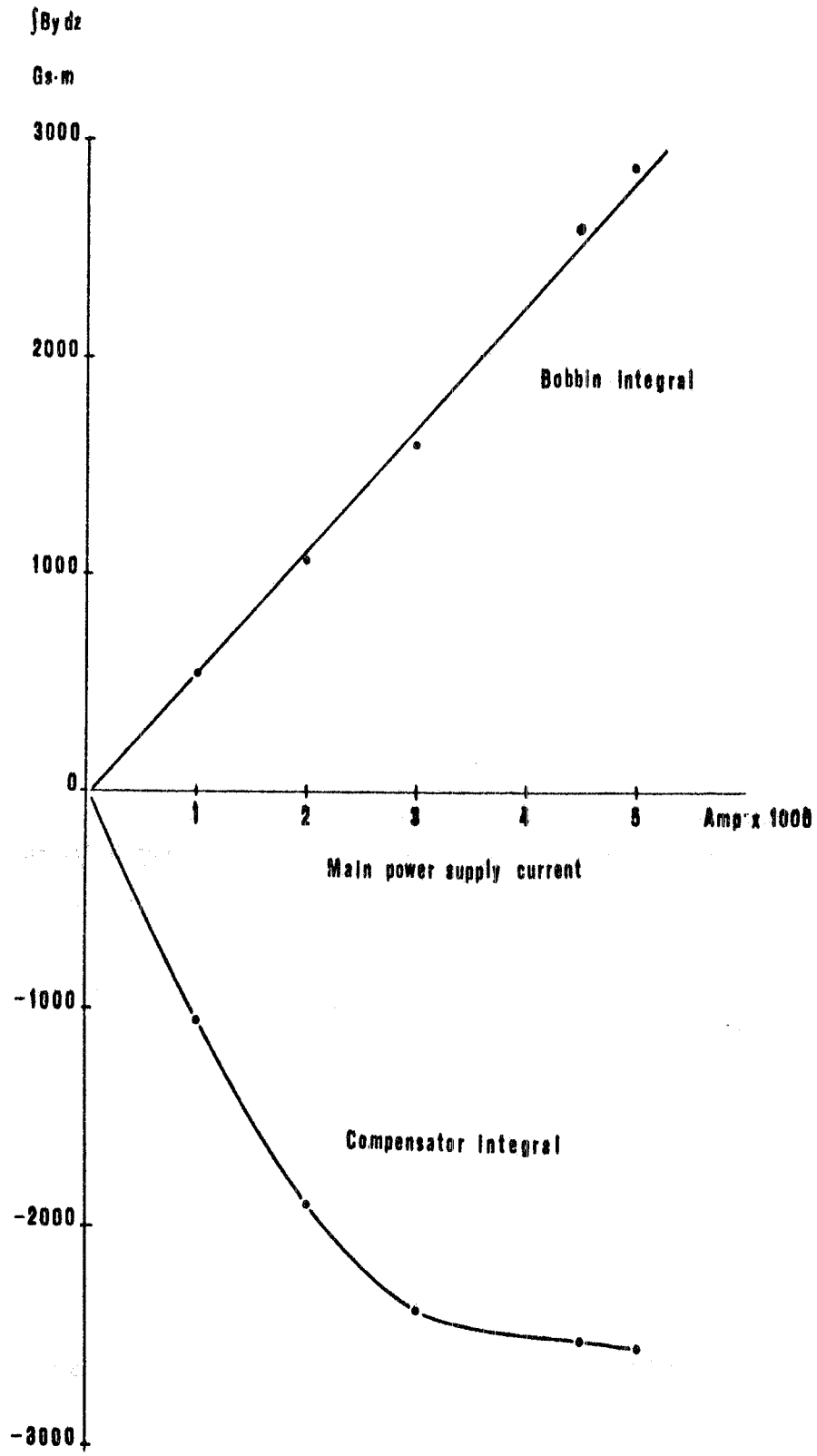

FIG. 5 - Field integral components vs current for the (uncompensated) initial configuration.

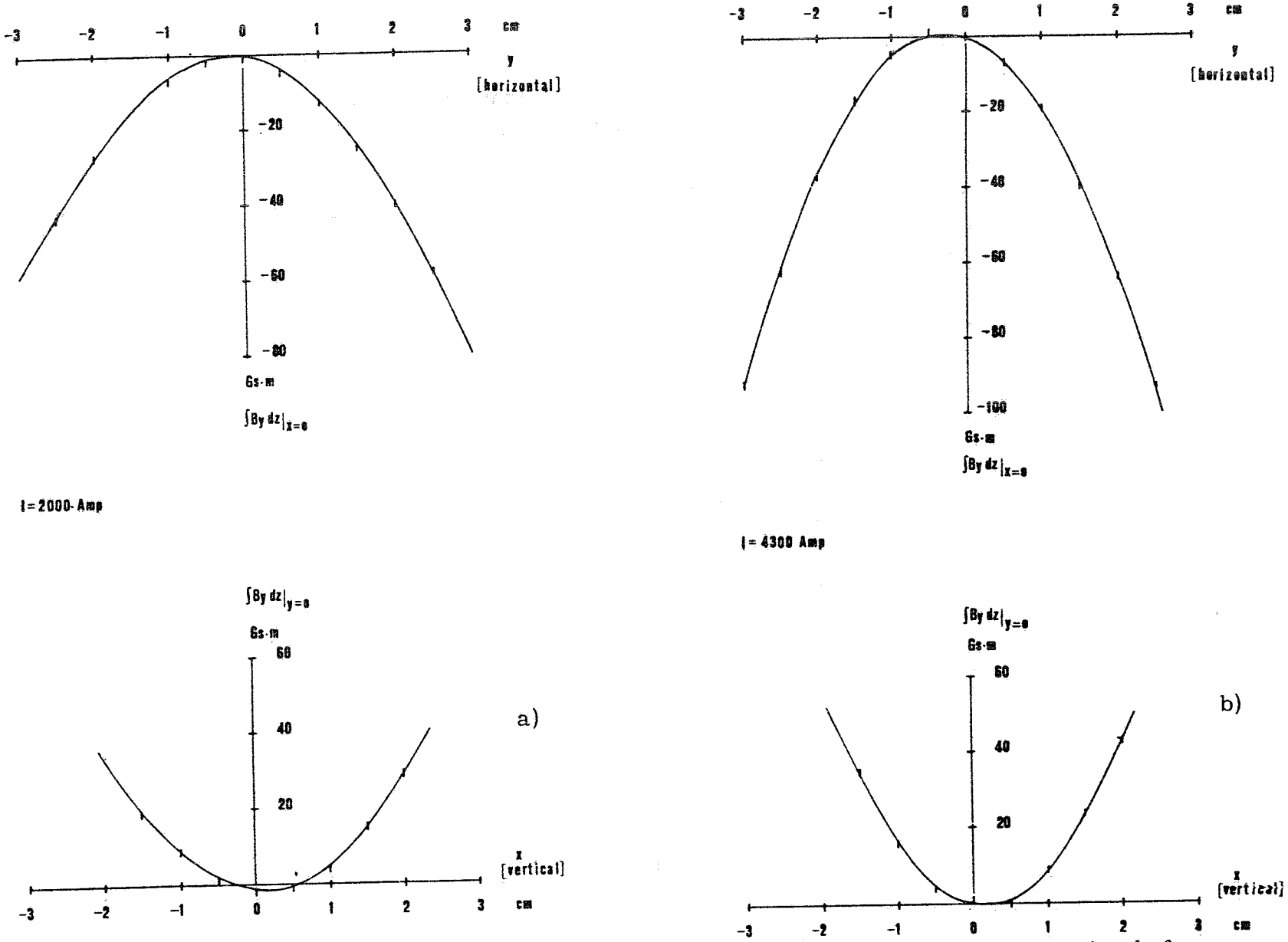

FIG. 6 - Horizontal and vertical field integral gradients in a compensated configuration before gradient correction modification a) 2000 amp. b) 4300 amp.

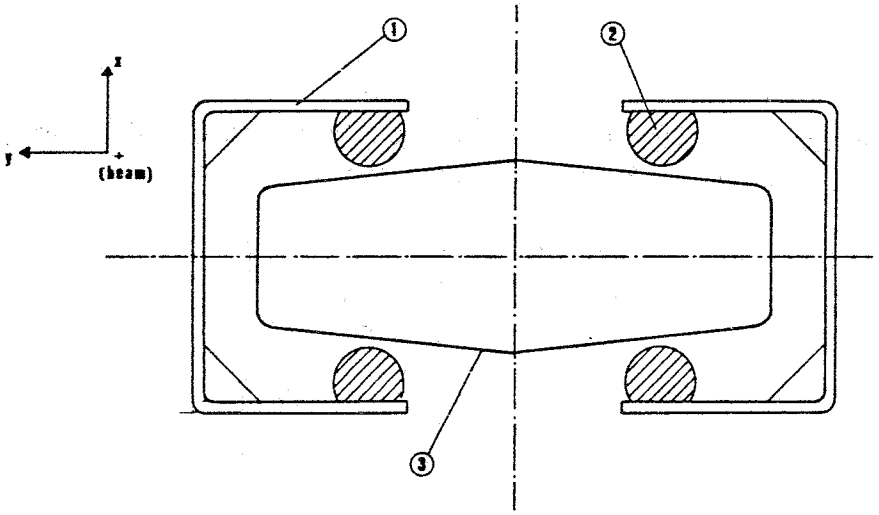

FIG. 7 - Details of the compensator insert for modifying field integral gradients. (1) aluminum support (2) one of four soft iron cylinders (3) Adone vacuum chamber.

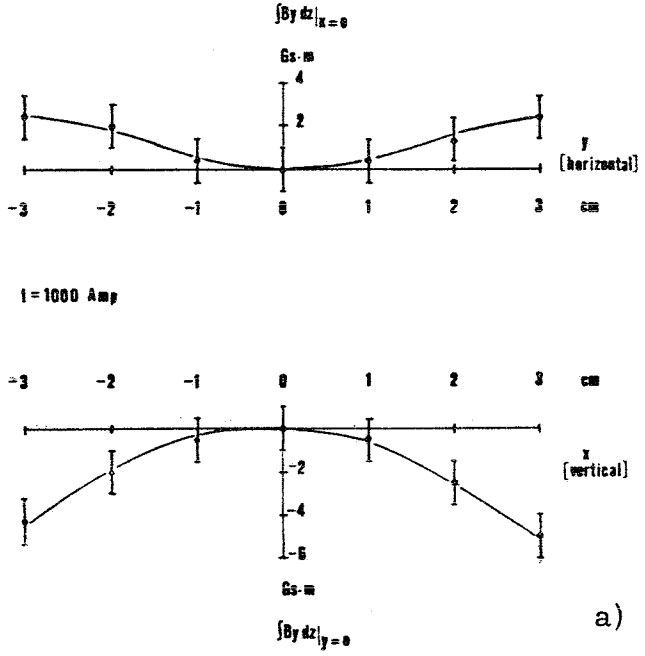

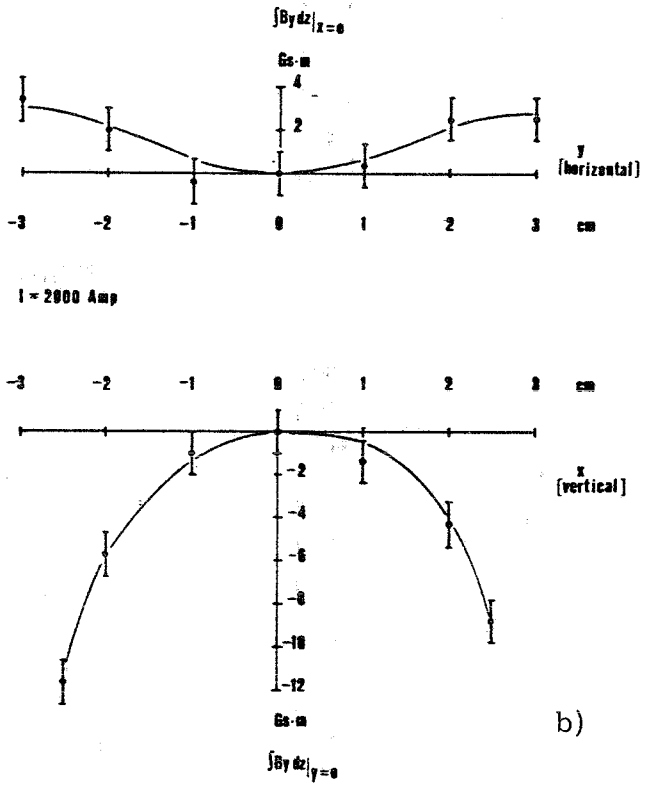

FIG. 8 - Horizontal and vertical field integral gradients in the final configuration (after modifications) a) 1000 amp. b) 2000 amp.

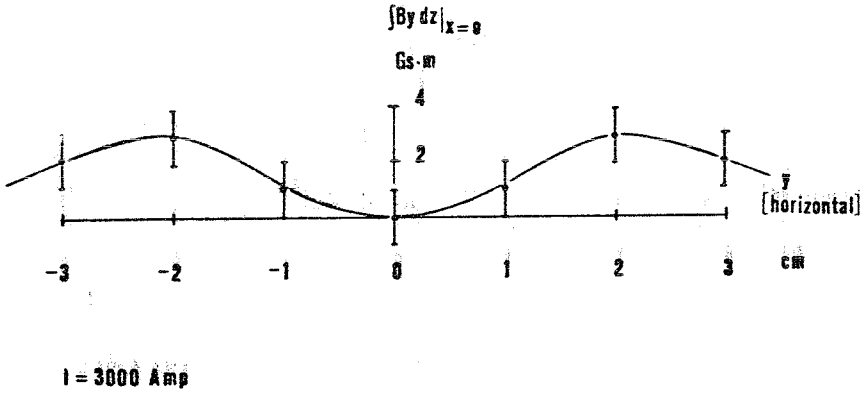

I = 3000 Amp

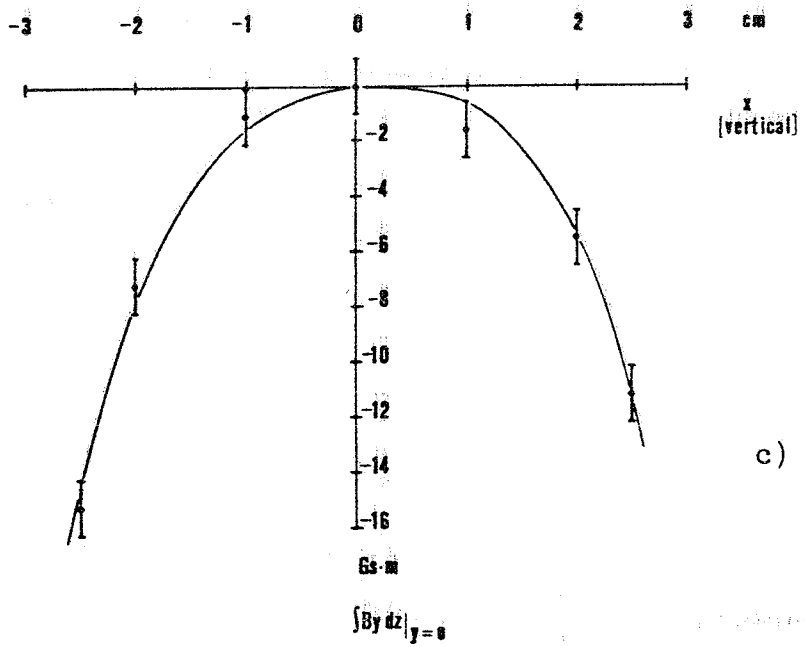

c)

FIG. 8 - c) 3000 amp.

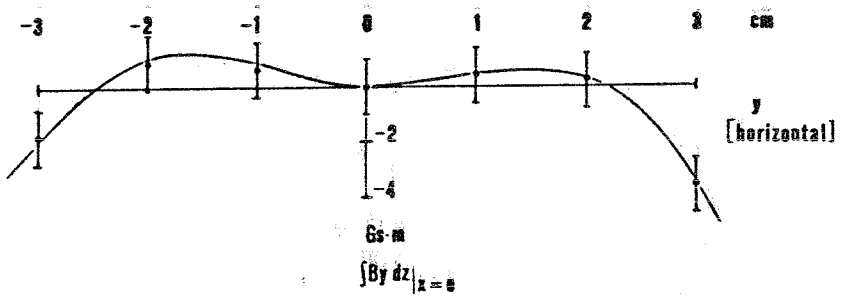

I = 3500 A

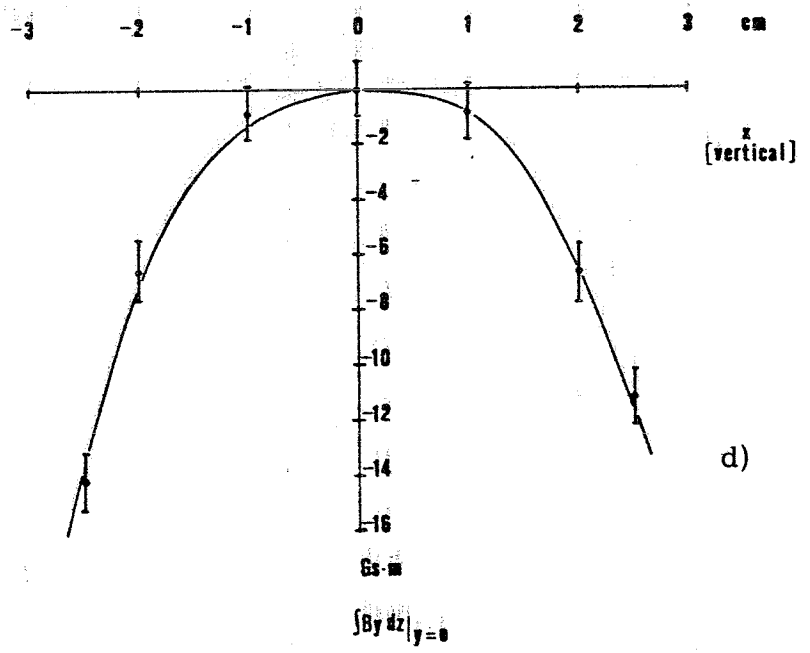

d)

FIG. 8 - d) 3500 amp.

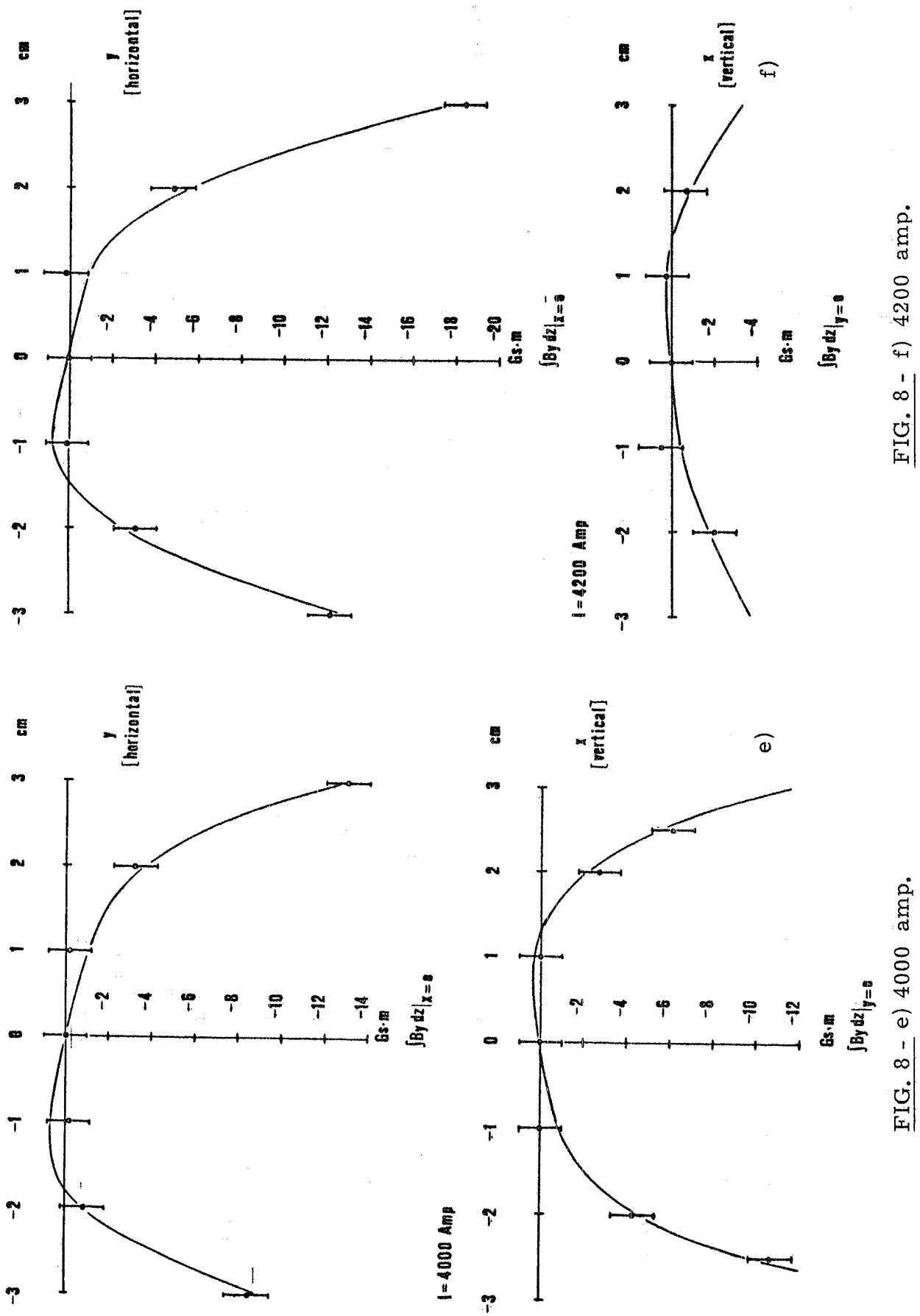

FIG. 8 - e) 4000 amp.

FIG. 8 - f) 4200 amp.

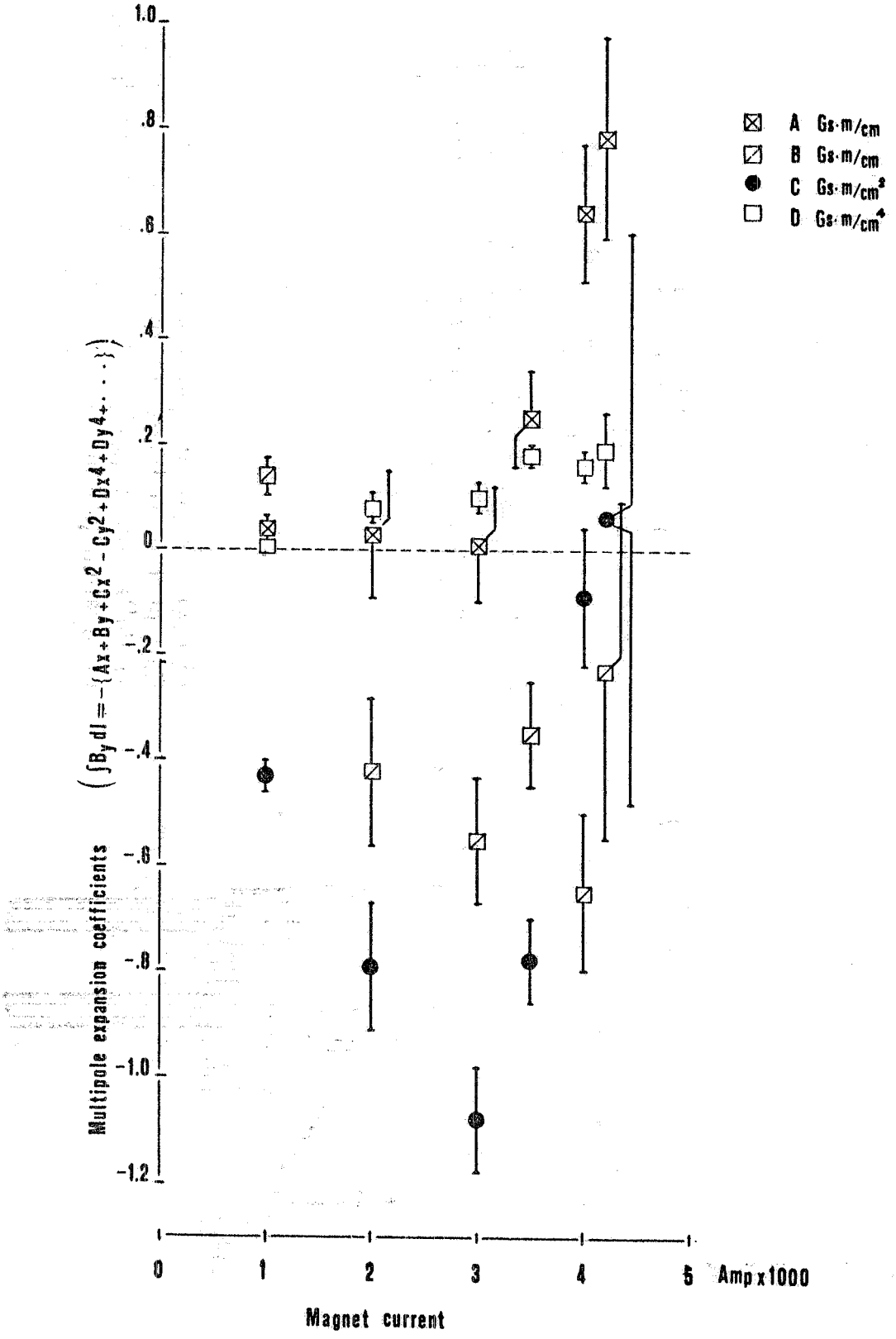

FIG. 9 - Multipole expansion coefficient vs main magnet current.

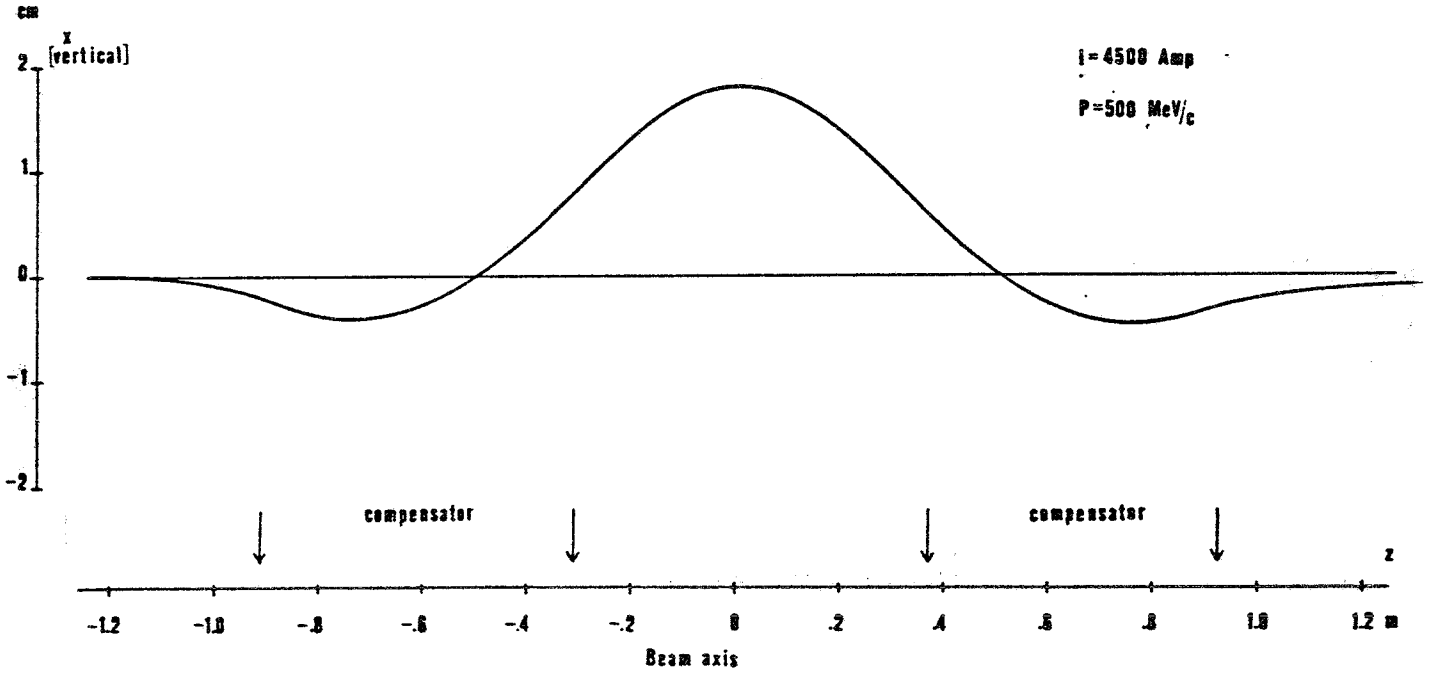

FIG. 10 - Beam trajectory within MEA straight section calculated from transverse profile at 4500 amp for a beam momentum of 500 MeV/c.

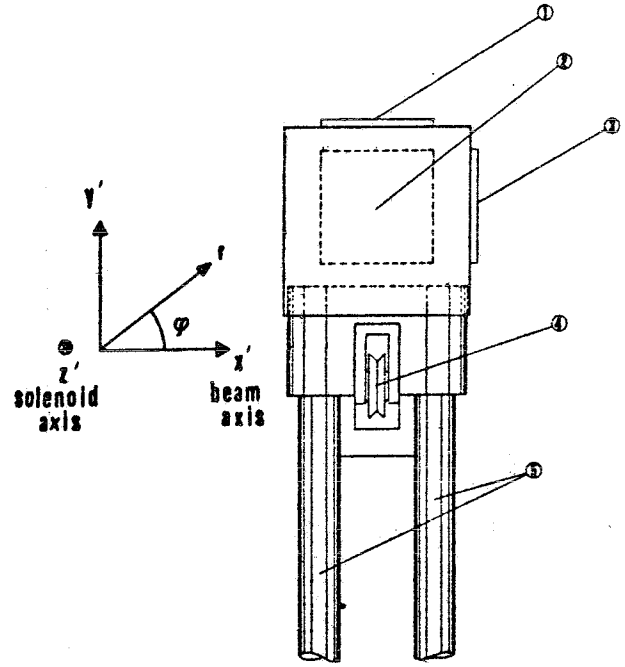

FIG. 11 - Field Mapper measuring head. 1) B_r Hall probe. 2) B_z Hall probe. 3) $B\varphi$ Hall probe. 4) Pulley for r position measurement. 5) Hydraulic system pistons for r movement.

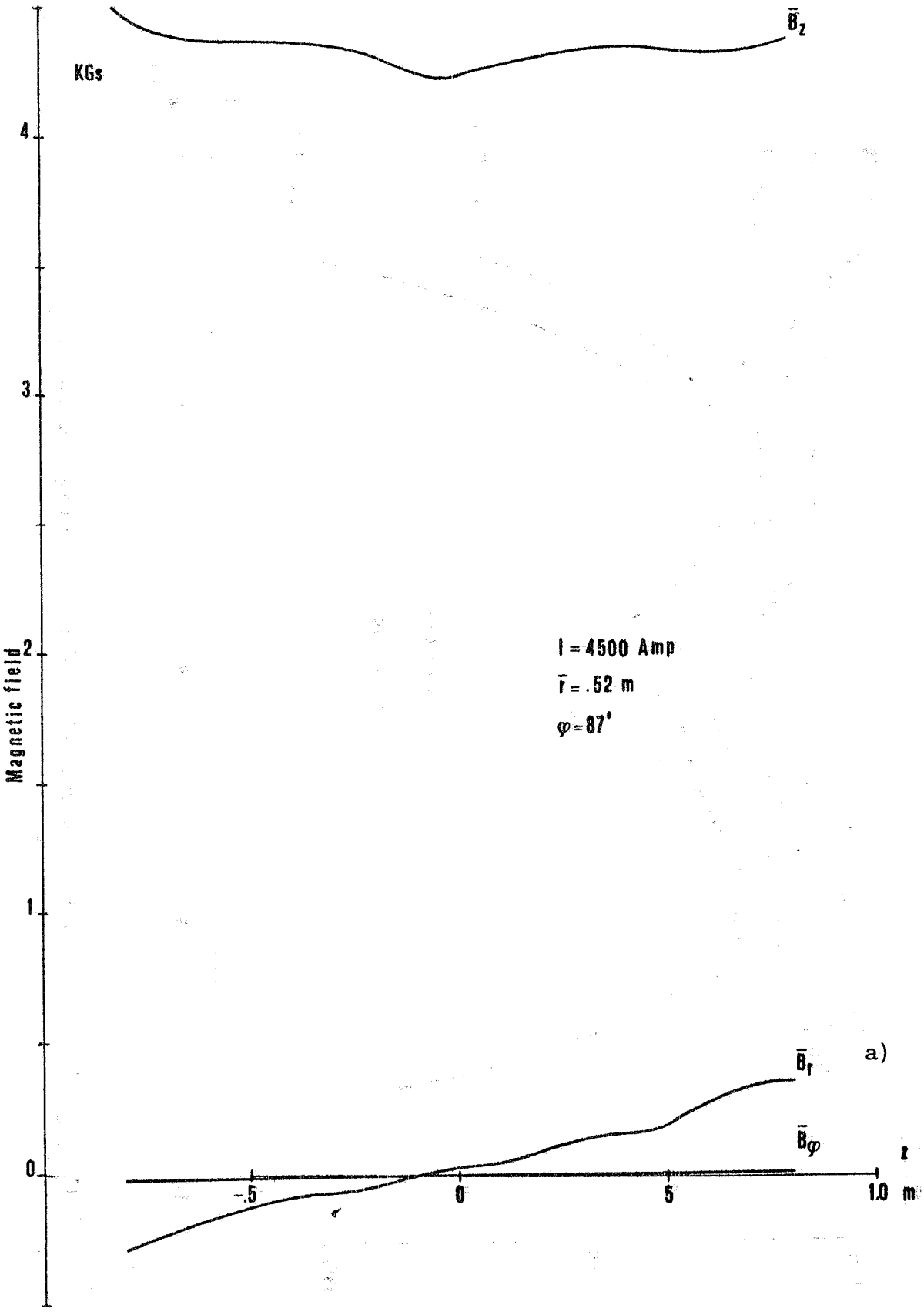

FIG. 12 - Principle projections of solenoidal magnetic field at 4500 amp. a) B_z, B_r, B_φ vs z (Axial coordinate) for 0.47 m < < r < 0.57 m and $78^o < \varphi < 96^o$.

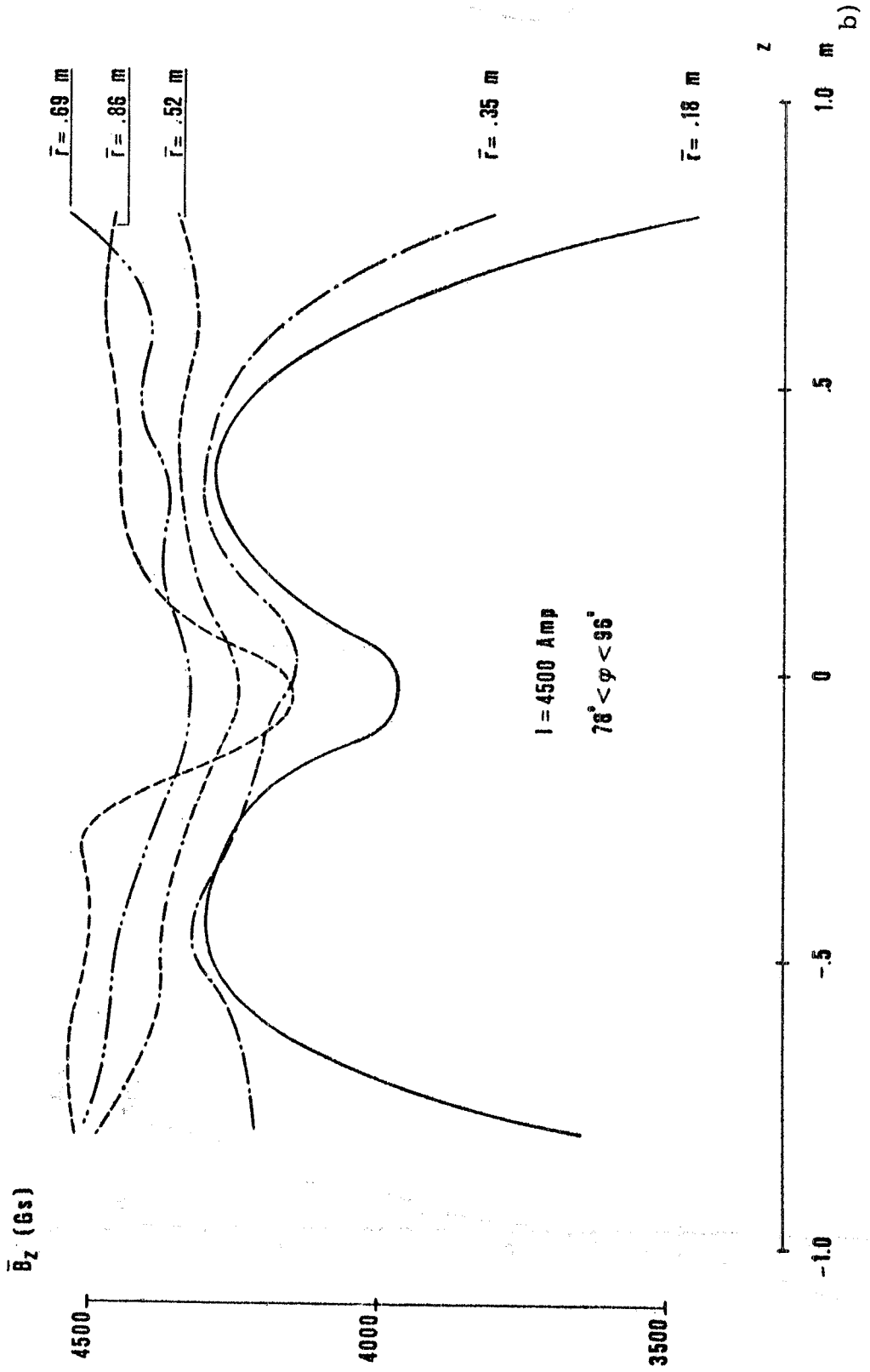

FIG. 12 - b) B_z vs Z for ($78° < \varphi < 96°$) and for 5 average values of r.

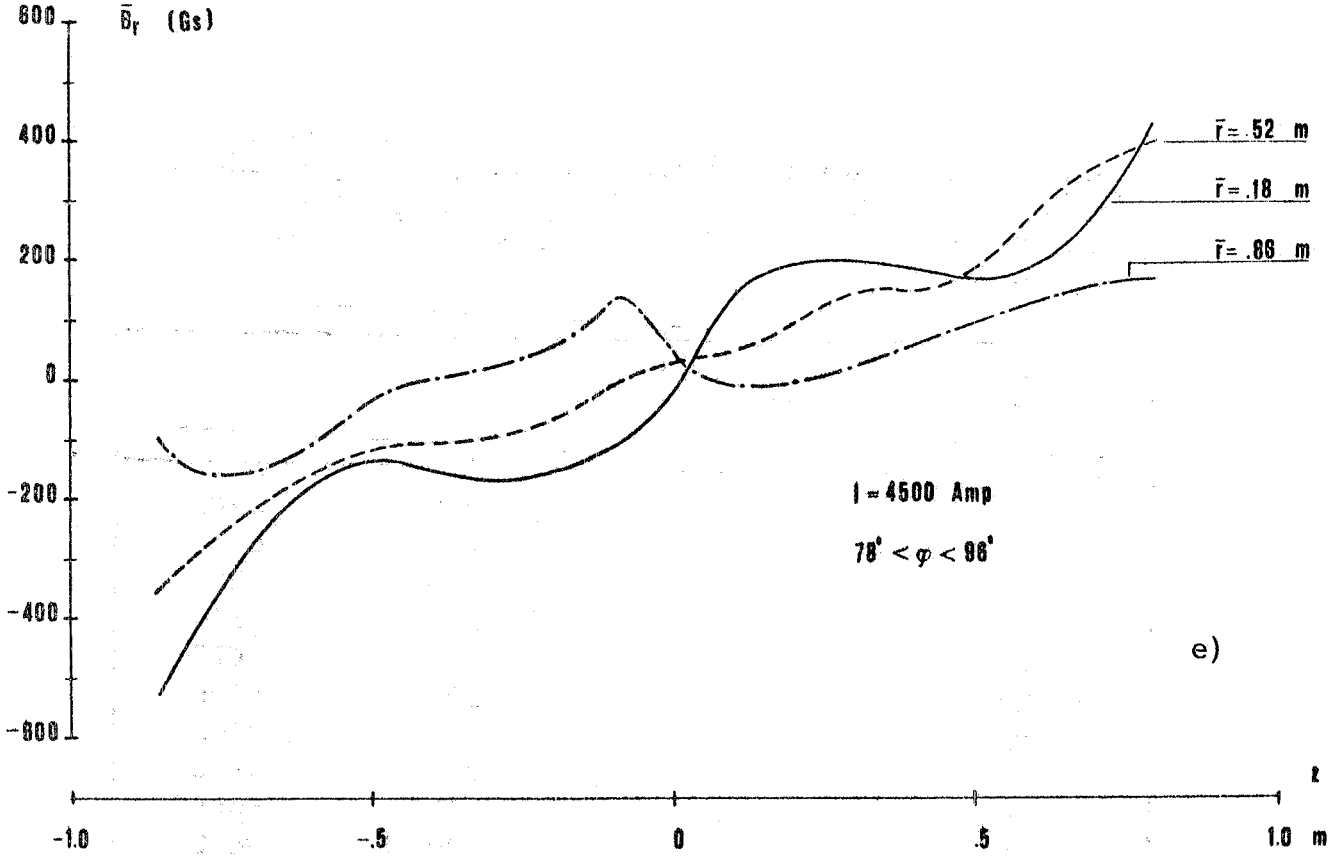

FIG. 12 - c) B_r vs Z for $78^\circ < \varphi < 96^\circ$ and 3 average values of r.

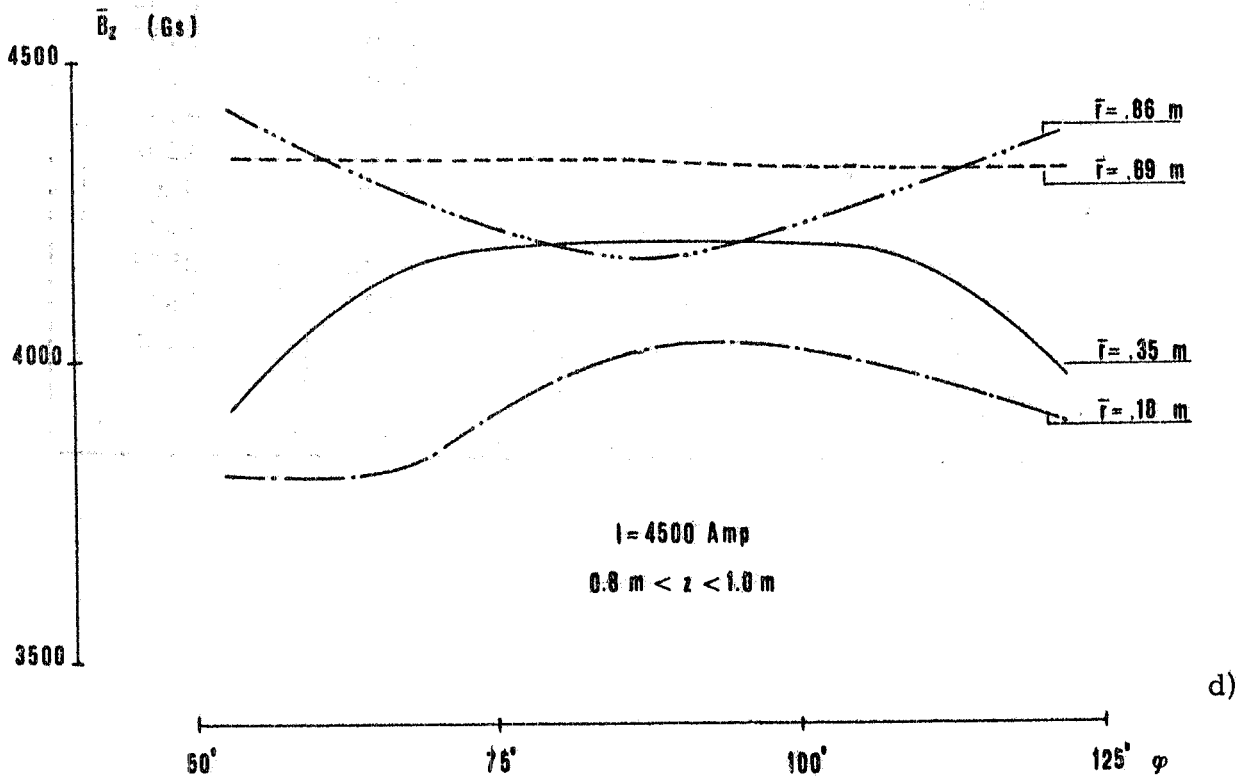

FIG. 12 - d) B_z vs φ for 0.8 m < Z < 1.0 m and for 4 average values of r.

TABLE I - Zero integral conditions. The reference voltage (0.1 volts = 5 amps) for the correction coil power supply is listed for the full range of magnet currents for the zero integral condition.

I (amps) Main power supply current	V (mvolts) Reference voltage	I	V
0	31.	2400	5991
100	370.	2500	6187
200	622.	2600	6372
300	851.	2700	6516
400	1102.	2800	6627
500	1350.	2900	6696
600	1583.	3000	6703
700	1842.	3100	6648
800	2100.	3200	6559
900	2347.	3300	6432
1000	2608.	3400	6220
1100	2866.	3500	6039
1200	3125.	3600	5760
1300	3375.	3700	5457
1400	3622.	3800	5131
1500	3871.	3900	4741
1600	4123.	4000	4289
1700	4366.	4100	3800
1800	4607.	4200	3237
1900	4846.	4300	2593
2000	5085.	4400	1910
2100	5315.	4500	1129
2200	5555.		
2300	5784.		

TABLE II - Multipole expansion coefficients ($\int B_y dl = -(Ax + By + Cx^2 - Cy^2 + Dx^4 + Dy^4 + Ex^6 - Ey^6 + Fx^8 + Fy^8)$).
a) Initial compensator configuration. - b) Final compensator configuration after all modifications.

a)

	A Gs m/cm	B Gs m/cm	C Gs m/cm^2	D Gs m/cm^4	E Gs m/cm^6	F Gs m/cm^8	χ^2 (D. of F. = 4)
2000 A	3.16 ± 0.24	1.63 ± 0.45	8.2 ± 0.3	0.14 ± 0.08	0.0024 ± 0.0270	0.00464 ± 0.00470	1.45
4300 A	6.71 ± 0.21	3.64 ± 0.41	12.8 ± 0.30	0.036 ± 0.041	0.016 ± 0.018	-0.0017 ± 0.0018	1.30

b)

	A Gs m/cm	B Gs m/cm	C Gs m/cm^2	D Gs m/cm^4	E Gs m/cm^6	F Gs m/cm^8	χ^2 (4 degrees of freedom)
1000 A	0.04 ± 0.03	0.14 ± 0.03	-0.43 ± 0.03	0.010 ± 0.007	-0.003 ± 0.001	0.0005 ± 0.0001	0.02
2000 A	0.03 ± 0.12	-0.42 ± 0.14	-0.79 ± 0.12	0.08 ± 0.03	-0.006 ± 0.003	0.0002 ± 0.0006	0.4
3000 A	0.01 ± 0.10	-0.55 ± 0.12	-1.08 ± 0.11	0.10 ± 0.03	-0.006 ± 0.003	0.0006 ± 0.0005	0.3
3500 A	0.25 ± 0.09	-0.35 ± 0.10	-0.78 ± 0.09	0.18 ± 0.02	-0.004 ± 0.002	-0.0003 ± 0.0004	0.2
4000 A	0.64 ± 0.13	-0.65 ± 0.14	-0.09 ± 0.13	0.16 ± 0.03	-0.004 ± 0.004	0.0001 ± 0.0006	0.5
4200 A	0.78 ± 0.19	-0.23 ± 0.32	0.06 ± 0.54	0.19 ± 0.07	0.015 ± 0.035	-0.0019 ± 0.0039	1.06

TABLE III - Beam displacement at magnet center (straight section center). Displacements are shown for seven current values under zero integral conditions as a function of beam momentum.

I (Amp)	P (MeV/c)	Central vertical displacement (mm)
4500	500	18
	1000	9
	1500	6
4300	500	17
	1000	9
	1500	6
4000	500	16
	1000	8
	1500	5
3700	500	14
	1000	7
	1500	5
3500	500	14
	1000	7
	1500	5
3000	500	12
	1000	6
	1500	4
2000	500	8
	1000	4
	1500	3

TABLE IV - Parameter determination from fit to magnetic field measurements. Each component was fit with the following functional form : $B_{z,r,\varphi} = B(1)+B(2)\cos\varphi + B(3)(1-R^2)(1-Z^2)\cos^2\varphi + B(4)R^2\cos^2\varphi + B(5)Z + B(6)Z\cos^2\varphi + B(7)ZR^2 + B(8)ZR^2\cos^2\varphi + B(9)Z^2 + B(10)Z^2\cos^2\varphi + B(11)Z^2R^2 + B(12)Z^2R^2\cos^2\varphi + B(13)Z^4 + B(14)(1/((Z^2+0.04)\cdot(R^2+0.04))) + B(15)Z^4R^2 + B(16)\cos\varphi^2/((Z^2+0.04)((R-0.5)^2+0.1)) + F_D(B(17), B(18)) + F_C(B(19), B(20))$. F_D is a field resulting from two symmetric magnetic dipoles with distances $x = \pm B(17)$ and equal dipole constants B(18). F_C is the field resulting from 8 single coils at Z=0, R=1.06 m and Z= $\pm$1.0 m, R=0.45 m with currents $B(19)_{Z=0}$ and $B(20)_{Z=\pm1}$. In addition we have indicated the fitting errors for each parameter to indicate the sensitivity of the fit to each functional form and $\Delta B = \sqrt{\Sigma(B_{meas} - B_{calc})^2/N.\ points}$.

a) 2000 amps; b) 3000 amps; c) 3000 amps (repeated measurement); d) 3500 amps; e) 3700 amps; f) 4000 amps; g) 4000 amps (repeated); h) 4000 amps (displaced correction coil current); i) 4300 amps; j) 4500 amps.

Upper half. Current 2000 Amps
Correction R volts 5.105
Record numbers 177-187

Par.	B_Z	B_R	$B\varphi$
1	2102.6±1.4	9.4797±.4943	-6.4495±.9059
2	1.1734±.4122	1.4972±.4113	-.03265±.77627
3	-10.095±4.787	-23.489±3.606	-54.898±6.984
4	-15.523±4.426	-10.031±3.241	5.6251±6.4671
5	1.2059±1.292	.60202±2.1350	10.944±1.858
6	-5.1689±5.6001	30.656±4.712	24.207±8.304
7	-11.364±2.426	53.377±2.888	-18.769±3.631
8	1.0077±10.626	-40.519±8.742	-23.978±16.059
9	-228.43±7.46	3.8224±4.6562	43.081±8.6807
10	-52.289±9.609	52.294±8.7173	25.531±14.984
11	194.26±9.88	-18.587±6.851	-52.621±13.54
12	86.065±19.633	-68.797±16.255	-7.0489±30.440
13	215.95±9.565	-30.872±7.638	-53.605±14.070
14	-.11165±.00688	.03053±.00368	.00149±.00627
15	-267.94±15.217	47.329±12.215	50.343±23.672
16	.30005±.03975	.17047±.02124	.09902±.041189
17	.41258±.001238	.39293±.00158	.37529±.001835
18	10.346±.170	9.7323±.1251	7.9216±.10566
19	-27095±189	-30236±180	0
20	-8895±116.4	-10252±86	0
$\overline{\Delta B}$	7.2	6.2	11.6

Lower half. Current 2000 Amps
Correction R volts 5.105
Record numbers 33-44

Par.	B_Z	B_R	$B\varphi$
1	2087.6±1.50	7.0776±.543	2.5523±1.0516
2	-1.0557±.4159	.18788±.43667	11.627±.865
3	-45.361±4.3554	-23.893±3.533	-88.885±7.287
4	-24.290±5.155	1.8123±3.9266	-11.754±8.291
5	-8.1150±1.1584	23.501±2.059	17.245±1.903
6	-.07483±5.0867	17.914±4.507	5.457±7.856
7	5.5480±2.5662	53.670±3.020	-23.286±4.355
8	7.4495±11.288	-66.493±9.771	-60.341±18.326
9	-197.76±7.847	-13.128±4.710	11.485±9.090
10	-31.616±8.8519	12.750±8.266	110.32±15.03
11	201.41±11.001	4.2370±7.6483	57.656±15.94
12	116.99±21.267	-54.745±18.015	-133.76±36.11
13	160.62±10.039	43.953±7.578	-12.868±14.67
14	-.07039±.006118	.012461±.00369	-.03879±.00676
15	-270.31±16.942	-63.122±13.445	-94.099±27.631
16	.48344±.03772	.13891±.02118	.19709±.04028
17	.41538±.00115	.38545±.00152	.38128±.00238
18	10.539±.158	9.1078±.1202	7.3279±.1046
19	-28471±198	-29252±171	0
20	-6975.1±139	-8279±107	0
$\overline{\Delta B}$	7.3	6.5	12.9

b) Upper half. Current 3000 Amps
Correction R volts 6.686
Record numbers 133-143

Par.	B_Z	B_R	$B\varphi$
1	3149.3±3.7	18.678±.799	-2.8803±1.6831
2	-8.1511±.9668	9.0794±.6234	8.0200±1.4064
3	-51.621±8.613	9.3743±4.0791	36.278±9.6442
4	-30.459±12.199	-41.656±5.6084	66.739±13.263
5	-4.9665±3.0657	-25.204±3.3077	21.287±3.2773
6	-24.947±13.408	45.315±7.4403	-10.317±14.347
7	-8.4697±6.4548	110.74±4.5836	-42.749±7.0828
8	35.522±27.559	-90.726±14.808	50.497±30.483
9	-339.34±22.69	-68.189±7.9069	-43.048±16.377
10	-57.932±25.22	-16.009±13.926	39.414±29.051
11	178.89±29.71	87.917±11.453	-104.44±26.086
12	-2.1858±54.638	67.988±27.992	-198.92±63.803
13	213.41±29.184	168.83±12.614	34.806±25.803
14	-.09788±.01259	-.02279±.00409	-.07816±.007965
15	-177.71±45.962	-271.14±21.184	181.57±46.939
16	.89859±.08022	-.03102±.0273	-.46105±.0553
17	.43077±.001588	.39621±.001302	.37857±.00164
18	17.901±.39226	15.0943±.17016	11.905±.15761
19	-43799.8±574.8	47645±313	0
20	-15544±316.6	-16493±143	0
$\overline{\Delta B}$	14	8.5	18

Lower half. Current 3000 Amps
Correction R volts 6.686
Record numbers 45-55

Par.	B_Z	B_R	$B\varphi$
1	3108.7±4.7	12.415±.842	4.0254±1.5371
2	-11.2014±1.3708	.8742±.6677	21.104±12.528
3	-12.095±15.141	-34.009±5.3119	-62.318±9.924
4	-57.360±16.072	34.128±6.0009	-2.444±10.755
5	3.6915±3.9381	41.465±3.1240	21.806±2.7656
6	-61.367±17.318	17.950±7.222	-15.747±12.081
7	-12.685±8.785	77.094±4.6775	-30.949±6.406
8	70.835±39.769	-79.991±15.923	19.394±28.062
9	-327.96±24.720	-26.347±7.2072	-34.658±13.093
10	-265.80±30.027	27.197±13.239	96.298±22.342
11	304.41±34.11	3.7184±11.777	146.41±22.95
12	506.84±68.81	-96.119±27.921	-123.89±49.73
13	339.28±30.787	31.135±11.633	67.976±21.31
14	-.16794±.02182	.01815±.006131	-137.43±.0103
15	-541.63±51.481	5.4856±20.693	-225.66±40.68
16	.49515±.12734	.12349±.03213	-.17972±.05803
17	.421618±.00259	.37889±.001566	.37696±.00183
18	15.4205±.56107	12.319±.17101	11.445±.1356
19	-43582±576	-42935±258.7	0
20	-9490.1±406.1	-11152±169.1	0
$\overline{\Delta B}$	23	10	18.5

Upper half. Current 3000 Amps
Correction R volts 6.686
Record numbers 188-195

Par.	B_Z	B_R	$B\varphi$
1	3138.9±3.3	12.982±.9119	-10.034±1.4598
2	-2.5279±.93301	.5809±.7919	-.99407±1.247
3	-46.929±10.269	-24.669±6.479	-26.672±9.0165
4	-5.9279±10.777	-12.735±6.4254	51.856±11.522
5	-7.0515±2.6678	-12.292±3.735	22.798±2.833
6	-33.733±12.132	21.156±8.346	16.111±12.847
7	-5.8915±5.4539	101.79±5.152	-43.269±5.985
8	34.892±24.328	-44.325±16.201	8.5788±26.263
9	-326.181±18.543	-40.824±8.6139	92.239±13.837
10	16.636±21.3083	92.369±16.117	59.473±23.387
11	220.59±23.59	71.866±12.808	-170.14±21.915
12	-99.047±46.99	-128.37±31.962	-143.62±52.615
13	182.17±24.42	51.089±14.466	-157.31±23.174
14	-1.0093±.01459	.02513±.00591	-.01896±.00887
15	-162.24±.00383	-114.94±23.95	280.05±40.592
16	.64922±.08750	.11192±.03942	-.15802±.06036
17	.42975±.001916	.38696±.001588	.37721±.00167
18	17.302±.4469	14.497±.21087	12.339±.15253
19	-41488±446	-46823±350	0
20	-13718±269	-15734±163	0
$\overline{\Delta B}$	14	11	18

Lower half. Current 3000 Amps
Correction R volts 6.686
Record numbers 100-111

Par.	B_Z	B_R	$B\varphi$
1	3107.9±3.1481	12.816±.7489	12.328±1.291
2	-6.6758±.83169	3.8364±.59714	20.479±1.0579
3	-119.42±8.222	-31.778±4.305	139.58±8.4892
4	-75.172±10.932	-8.4983±5.6224	-30.617±10.780
5	-14.508±2.358	33.710±2.8564	29.410±2.3347
6	21.957±10.689	44.900±6.4515	-9.7696±10.210
7	11.292±5.4383	101.21±4.2918	-42.033±5.6091
8	-23.336±24.323	-171.87±14.147	-35.147±24.242
9	-335.96±16.773	-18.037±6.7104	-95.664±11.417
10	13.208±18.847	66.629±11.534	-86.055±19.104
11	320.97±23.524	-4.4823±10.961	161.61±20.453
12	150.42±47.012	-133.94±26.497	173.54±48.167
13	250.41±20.407	22.579±10.027	160.41±17.29
14	-.06261±.01202	.0022612±.0047	-.10101±.00767
15	-414.79±37.447	-15.103±19.652	-301.76±36.238
16	1.3009±.07105	.107340±.02473	-.53518±.04166
17	.43043±.00145	.38113±.00129	.37023±.001515
18	17.395±.34787	12.982±.1466	10.326±.1163
19	-42489±411	-42839±219	0
20	-10548±289	-12599±147	0
$\overline{\Delta B}$	12.8	8.5	15

d) Lower half. Current 3500 Amps
Correction R volts 6.007
Record numbers 56-66

Par.	BZ	BR	Bφ
1	3608.2±2.8	13.184±1.0629	6.424±1.904
2	-6.4692±.7921	6.8763±.8499	23.965±1.522
3	-45.482±8.091	-53.033±6.2338	-84.734±11.006
4	-50.929±10.320	66.779±8.4419	24.249±14.342
5	-9.3171±2.224	46.000±3.6368	35.794±3.271
6	-19.705±9.9501	16.9279±8.8498	-11.508±14.314
7	-.3041±5.8473	99.555±6.1664	-68.229±8.787
8	25.991±26.581	-114.81±22.404	63.917±38.639
9	-415.26±15.163	-14.354±8.909	-1.1907±15.855
10	-52.992±17.941	70.793±16.637	180.67±27.796
11	417.76±22.611	1.39043±15.967	151.34±31.017
12	120.89±46.235	-220.16±39.650	-352.65±68.824
13	347.48±19.608	10.885±14.887	-22.800±26.863
14	-.12105±.011691	.02015±.006932	-.05308±.011506
15	-552.87±346	28.748±28.779	-151.97±56.84
16	.77065±.06928	.10396±.03897	-.22798±.0701
17	.41648±.00126	.37613±.00159	.37478±.00188
18	17.336±.299	13.997±.1979	11.818±.157
19	-49381±390	-50174±308	0
20	-10496±249	-13471±244	0
$\overline{\Delta B}$	13.6	12	21.8

Upper half. Current 3700 Amps
Correction R volts 5.437
Record numbers 144-154

Par.	B_Z	B_R	$B\varphi$
1	3850.6±3.7	20.103±1.1143	31.124±1.80
2	-7.6500±.9928	7.6966±.8812	9.6518±1.4673
3	-107.82±9.18	.35575±5.9184	116.13±11.58
4	-64.244±13.146	-54.427±8.283	21.548±14.885
5	.30553±2.9731	-13.273±4.339	23.475±3.250
6	-39.079±12.784	113.60±9.569	-1.2661±13.715
7	-24.322±6.804	152.34±6.56	-44.848±7.802
8	74.666±28.858	-233.29±20.83	43.129±32.542
9	-588.12±20.041	-49.139±10.182	-86.747±16.508
10	-120.97±22.74	88.958±17.253	-110.59±27.06
11	529.92±28.29	89.075±16.248	-95.581±28.719
12	261.89±55.71	-98.894±38.823	75.732±66.354
13	512.85±24.38	25.986±15.264	115.85±24.794
14	-.03134±.01329	-.01971±.00634	-.12983±.00973
15	-713.50±44.71	-91.359±29.005	133.92±50.10
16	1.6215±.0825	.01629±.03634	-.3085±.05750
17	.42957±.00131	.39464±.00155	.35923±.00182
18	21.833±.391	17.107±.228	11.077±.151
19	-48911±480	53201±333	0
20	-18434±331	-21047±211	0
$\overline{\Delta B}$	15.6	12.3	20

Lower half. Current 3700 Amps
Correction R volts 5.437
Record numbers 112-120

Par.	B_Z	B_R	$B\varphi$
1	3807.3±3.5	18.088±.897	14.987±1.638
2	-6.9532±.9544	5.5630±.6584	24.128±1.295
3	-72.984±12.759	-15.434±5.4517	57.585±8.997
4	-70.367±12.456	-12.107±6.6818	-34.339±13.063
5	-17.291±2.689	61.589±3.3018	33.597±2.884
6	13.119±11.970	61.023±7.274	-2.5163±12.360
7	7.5471±6.152	118.71±4.93	-47.998±6.867
8	11.194±26.994	-227.15±15.917	-52.139±28.980
9	-479.11±18.182	-58.006±7.695	-95.686±13.630
10	-20.006±22.195	52.437±13.796	-1.0595±23.261
11	505.89±26.130	29.532±12.807	156.84±24.429
12	175.96±54.616	-135.04±31.61	59.821±58.203
13	390.89±22.44	109.03±11.85	158.34±20.800
14	-.12565±.01888	-.010529±.007971	-.15925±.01314
15	-668.46±42.339	-118.40±23.27	-297.04±43.58
16	1.16618±.09706	.027451±.029583	.089064±.051517
17	.416221±.001804	.35884±.00157	.36120±.00217
18	17.648±.434	12.648±.166	10.756±.147
19	-51003±446	-50893±255	0
20	-12289±321	-15173±168	0
$\overline{\Delta B}$	15.1	10.5	18.7

f) Upper half. Current 4000 Amps
Correction R volts 4.255
Record numbers 155-165

Par.	B_Z	B_R	$B\varphi$
1	4158.6±3.6	20.857±1.064	20.420±2.4311
2	-5.9769±.9203	7.7124±.8085	15.314±1.994
3	-94.504±9.528	16.388±5.9509	40.241±14.456
4	-72.294±13.339	-74.499±8.3618	30.539±20.981
5	-12.217±2.689	1.2977±3.9413	27.078±4.270
6	-9.7563±11.958	108.87±8.89	55.879±18.597
7	-8.9186±6.4960	141.82±5.960	-48.395±10.712
8	34.1519±28.092	-237.51±20.16	-69.224±45.475
9	-639.60±19.851	-90.228±9.378	-128.45±21.238
10	-109.43±22.275	-22.440±17.221	8.2006±37.758
11	531.62±28.494	138.91±15.524	-135.33±38.106
12	236.28±56.327	104.59±39.481	-183.16±93.96
13	505.52±24.607	209.83±14.68	161.16±33.149
14	-.030903±.013092	-.032066±.005944	-.17998±.01246
15	-673.12±45.246	-376.61±28.519	222.56±68.42
16	1.6230±.08765	.015673±.03748	.24588±.08408
17	.42620±.00125	.38578±.00137	.36599±.00217
18	22.418±.379	16.312±.2139	12.876±.199
19	-54939±472	-57661±338	0
20	-20227±322	-22263±209	0
$\overline{\Delta B}$	15.8	11.5	27

Lower half. Current 4000 Amps
Correction R volts 4.255
Record numbers 122-132

Par.	B_Z	B_R	$B\varphi$
1	4129.4±2.046	20.546±1.047	14.154±1.435
2	-5.6467±.6078	-3.2436±.8580	27.094±1.1381
3	-86.530±8.977	-57.889±8.9068	18.868±11.202
4	-42.713±6.555	10.522±6.6178	53.395±10.305
5	-9.9569±1.8973	22.795±4.349	26.758±2.849
6	-19.031±8.354	-36.120±9.5897	5.1088±12.745
7	-4.8598±3.5165	171.82±5.759	-30.910±5.443
8	35.534±15.519	-13.125±17.107	-77.769±23.971
9	-636.54±11.146	-59.895±10.009	-41.526±13.957
10	-95.606±14.634	118.28±18.295	43.747±24.074
11	646.84±14.122	39.327±14.392	47.282±21.358
12	199.44±29.76	-216.56±33.628	-129.72±49.157
13	606.16±15.18	102.41±16.95	65.980±23.822
14	-.06827±.01296	-.04668±.01193	-.08947±.01478
15	-956.10±23.25	-118.956±26.139	-92.041±38.942
16	1.1595±.06580	.20057±.04894	-1.0745±.06232
17	.42279±.00121	.34311±.00185	.31546±.00278
18	20.470±.323	13.108±.2027	10.1713±.1406
19	-56703±256	-60542±403	0
20	-13410±154	-16156±164	0
$\overline{\Delta B}$	11.4	13.0	18.2

Lower half. Current 4000 Amps
Correction R volts 4.255
Record numbers 68-78

Par.	B_Z	B_R	$B\varphi$
1	4119.0±2.5	19.283±1.032	9.3015±1.7114
2	-4.4145±.7022	1.9013±.8540	26.404±1.4325
3	-48.911±8.2110	-53.082±7.4667	-123.16±12.138
4	-50.823±8.434	13.9255±7.2841	1.9808±13.0613
5	-9.9610±2.1056	46.1386±4.0628	23.583±3.256
6	4.6580±9.1517	60.722±9.1579	42.957±14.885
7	-3.4603±4.3775	152.19±5.869	-31.705±7.0509
8	-2.6271±19.1468	-171.14±18.65	-121.00±31.606
9	-620.41±12.586	-38.484±9.2437	-2.3006±15.0148
10	-151.30±15.436	69.367±17.035	152.04±26.618
11	653.86±17.529	14.762±14.785	100.0±25.8
12	299.70±35.53	-165.64±35.163	-173.61±59.912
13	609.95±15.944	52.530±15.124	13.52±24.406
14	-.1352±.01140	-.02114±.00754	-.08004±.01176
15	-975.84±27.50	-53.288±26.422	-174.44±45.434
16	1.0251±.0686	.1779±.04185	-.03418±.07144
17	.41336±.00118	.36096±.00184	.3630±.00222
18	18.402±.296	13.574±.2103	10.502±.167
19	-55147±304	-56391±340	0
20	-13252±231.6	-16438±197	0
$\overline{\Delta B}$	12.9	13.1	22.0

h) Upper half. Current 4000 Amps
Correction R volts 3.255
Record numbers 12-21

Par.	B_Z	B_R	$B\varphi$
1	4162.8±3.8	19.757±1.236	-10.307±2.573
2	-2.4494±.9975	-2.0334±1.0067	3.9426±2.0945
3	-63.916±9.909	23.829±7.162	-19.123±14.062
4	-70.896±13.476	-26.185±9.317	92.394±21.611
5	-17.316±2.760	5.8086±4.2754	23.957±4.4217
6	32.176±12.695	64.623±10.271	65.459±20.549
7	4.3075±6.4597	136.06±6.62	-49.332±10.724
8	-55.762±28.952	-130.52±22.67	-27.291±47.983
9	-791.91±18.787	-84.033±10.424	90.068±21.942
10	-49.801±23.332	-32.506±19.569	106.21±39.696
11	703.71±25.457	118.51±17.098	-21.698±38.498
12	88.784±57.138	68.332±43.959	-325.96±97.732
13	704.81±23.80	160.66±16.774	-159.50±34.907
14	-.03978±.01429	-.00132±.00726	-.050535±.014143
15	-863.19±42.204	-277.90±31.03	366.90±68.453
16	1.29062±.08897	-.19049±.04659	-.12972±.09538
17	.426359±.001385	.37759±.00150	.366196±.001948
18	22.646±.424	16.156±.237	13.927±.2047
19	-51218±427	-56994±362	0
20	-19641±322	-21165±234	0
$\overline{\Delta B}$	17	13.6	29

i) Upper half. Current 4300 Amps
Correction R volts 2.637
Record numbers 22-32

Par.	B_Z	B_R	$B\varphi$
1	4460.2±4.0	23.999±1.358	6.8531±2.9591
2	4.4027±1.061	7.0014±.9849	6.9459±2.3772
3	-111.16±11.53	43.368±7.857	28.204±16.172
4	-84.806±14.808	-49.601±10.389	28.768±24.829
5	-16.650±2.9195	-6.5556±4.4983	22.006±4.835
6	38.286±12.679	118.11±10.416	99.676±20.947
7	2.0209±6.9979	176.51±7.0569	-47.243±12.209
8	-64.725±30.102	-227.48±24.002	-77.238±52.386
9	-869.40±19.45	-84.460±11.247	-55.497±24.216
10	-38.238±23.536	-91.931±20.033	-43.183±40.856
11	774.23±26.99	109.77±18.686	-129.28±43.42
12	68.618±60.024	155.26±46.952	9.5243±106.04
13	750.92±24.18	170.07±17.530	71.627±37.165
14	-.02832±.01629	.05247±.00908	-.14361±.01836
15	-945.55±45.41	-283.57±33.827	161.89±76.986
16	1.7351±.0990	-.19372±.04794	-.02137±.10215
17	.42841±.00145	.36810±.00164	.35809±.002217
18	23.818±.461	15.9808±.2485	13.178±.1902
19	-54919±428	-61654±369	0
20	-21142±355	-23268±256	0
$\overline{\Delta B}$	18	15.5	34

Lower half. Current 4300 Amps
Correction R volts 2.637
Record numbers 78-88

Par.	B_Z	B_R	$B\varphi$
1	4433.3±4.0	21.976±1.0236	23.175±2.170
2	3.6064±1.0626	5.9004±.7968	31.164±1.8020
3	-104.06±10.857	-21.664±5.477	134.79±12.067
4	-92.463±14.326	-24.259±7.753	-24.283±17.955
5	-2.1207±3.1386	45.914±3.908	34.930±3.8450
6	-20.873±13.953	94.435±8.9004	7.6020±17.492
7	-18.910±7.223	189.69±5.85	-47.905±9.2582
8	64.829±31.112	-313.61±19.12	-53.534±40.360
9	-774.67±20.787	-97.999±9.186	-173.33±19.336
10	-89.528±25.523	63.453±16.296	-50.689±33.796
11	745.86±29.243	81.070±14.686	223.86±33.299
12	313.16±61.78	-157.78±36.593	74.609±81.696
13	711.02±25.185	187.47±13.519	276.60±28.563
14	-.10586±.01539	-.04239±.005779	-.16734±.011256
15	-1064.4±47	-231.35±26.018	-403.43±58.04
16	1.6980±.0967	.051091±.03420	-.36917±.07098
17	.41854±.00146	.36672±.00127	.35376±.001946
18	20.879±.41708	14.519±.179	11.195±.18045
19	-57124±454	-59559±300	0
20	-15649±368	-18372±195	0
$\overline{\Delta B}$	17.2	11.4	24.4

Upper half. Current 4500 Amps
Correction R volts 1.100
Record numbers 0-11

Par.	B_Z	B_R	$B\varphi$
1	4652.3±3.6	21.847±1.225	-15.577±2.4354
2	4.9221±.9880	4.8395±1.0237	.12706±2.0666
3	-70.808±11.172	-16.364±8.7523	-83.793±15.801
4	-27.086±11.514	-27.322±8.465	118.47±18.741
5	-14.660±2.956	-9.1744±4.9456	23.071±4.7813
6	-17.480±13.013	62.7236±10.993	75.091±20.999
7	-9.3865±5.9383	187.90±6.8136	-48.302±9.9303
8	13.792±26.019	-107.26±21.22	-30.748±42.974
9	-802.11±19.459	-91.244±11.532	171.82±22.926
10	-100.93±23.008	128.27±21.32	186.13±39.75
11	675.01±24.807	138.09±17.08	-298.92±36.132
12	19.869±50.452	-155.37±41.96	-440.01±87.19
13	659.48±25.96	171.56±19.35	-312.04±38.48
14	-.05999±.01605	.012695±.00832	.011748±.015510
15	-819.86±40.535	-301.09±31.68	546.30±66.517
16	1.3602±.09331	.12674±.05305	-.34996±.101857
17	.41816±.00149	.36312±.00166	.345296±.0024313
18	21.813±.442	15.304±.2439	12.0178±.21360
19	-59532±459	-66171±469	0
20	-21313±308	-24160±216	0
$\overline{\Delta B}$	±17	15	31

Lower half. Current 4500 Amps
Correction R volts 1.100
Record numbers 89-99

Par.	B_Z	B_R	$B\varphi$
1	4607.6±3.8	20.928±1.154	18.223±1.954
2	-1.1353±1.0420	6.0170±.9251	31.339±1.611
3	-175.88±10.39	-38.096±6.801	219.51±12.89
4	-89.096±13.389	-11.479±8.512	-35.694±15.974
5	-25.030±3.015	41.645±4.4517	39.462±3.625
6	35.564±13.561	104.73±10.014	20.604±15.781
7	13.495±6.762	213.95±6.611	-56.239±8.465
8	-13.925±29.976	-324.30±21.35	-71.939±36.347
9	-690.84±20.783	-55.729±10.503	-149.29±17.492
10	-5.0849±23.467	73.474±17.844	-127.38±29.51
11	735.26±29.174	32.955±16.860	201.02±30.68
12	209.28±57.31	-159.33±40.137	183.93±72.17
13	550.97±25.771	99.613±15.735	242.89±26.45
14	-.046172±.015234	-.03915±.00729	-.15501±.01185
15	-1003.3±46.5	-126.25±30.219	-356.27±54.265
16	2.1108±.08846	.08218±.03865	-.75106±.06376
17	.413819±.00139	.35730±.001462	.33386±.00190
18	20.203±.393	14.129±.19314	9.3019±.15256
19	-61695±513	-62259±347	0
20	-14930±351	-19312±221	0
$\overline{\Delta B}$	18.6	13.5	23.2